The Journal of Experimental Biology 206, 2979-2987

doi:10.1242/jeb.00523

Flexural stiffness in insect wings

I. Scaling and the influence of wing venation

S. A. Combes* and T. L. Daniel

Department of Biology, University of Washington, Seattle, WA 98195, USA

*Author for correspondence (e-mail: scombes@u.washington.edu)

Accepted 3 June 2003

Summary

During flight, many insect wings undergo dramatic deformations that are controlled largely by the architecture of the wing. The pattern of supporting veins in wings varies widely among insect orders and families, but the functional significance of phylogenetic trends in wing venation remains unknown, and measurements of the mechanical properties of wings are rare. In this study, we address the relationship between venation pattern and wing flexibility by measuring the flexural stiffness of wings (in both the spanwise and chordwise directions) and quantifying wing venation in 16 insect species from six orders. These measurements show that spanwise flexural stiffness scales strongly with the cube of wing span, whereas chordwise flexural stiffness scales with the square of chord length. Wing size accounts for over 95% of the variability in measured flexural stiffness; the residuals of this relationship are small and uncorrelated with standardized independent contrasts of wing venation characters. In all species tested, spanwise flexural stiffness is 1–2 orders of magnitude larger than chordwise flexural stiffness. A finite element model of an insect wing demonstrates that leading edge veins are crucial in generating this spanwise–chordwise anisotropy.

Key words: insect flight, flexural stiffness, wing, wing flexibility, wing vein, independent contrast, finite element model.

Introduction

The forces generated during flapping flight depend on both the motion of a wing and its three-dimensional shape. Flying vertebrates, such as birds and bats, can control many aspects of wing shape by muscular contractions that alter the alignment of wing bones, the position of feathers or the tautness of wing membranes (Kent, 1992). Flying insects have far less active control over the three-dimensional shape of their wings, as insect flight muscles are restricted to the wing base. Insect wings are largely passive structures, in which muscular forces transmitted by the wing base interact with aerodynamic and inertial forces generated by the wing's motions. The architecture of the wing (vein arrangement, three-dimensional relief, flexion lines, etc.) and the material properties of its elements determine how the wing will change shape in response to these forces (Wootton, 1992).

Many insect wings undergo significant bending and twisting during flight (Dalton, 1975; Wootton, 1990a), which may alter the direction and magnitude of aerodynamic force production. Wing deformations enhance thrust production in some species by creating a force asymmetry between half-strokes, and can increase lift production by allowing wings to twist and generate upward force throughout the stroke cycle (Wootton, 1990a). The structure of insect wings thus appears to permit certain beneficial passive deformations while minimizing detrimental bending that would compromise force production. Yet our understanding of how insect wing design affects flexibility and passive wing deformation is limited.

Insect wing veins are the primary supporting structures in wings. The arrangement of veins and complexity of vein branching varies widely among insects, and venation pattern is often used to characterize orders and families. Basal groups of insects (such as odonates) generally possess wings with a large number of cross-veins (also present in early fossil wings), whereas more derived groups have wings in which the number of cross-veins is reduced and the main wing support is shifted anteriorly (Wootton, 1990a).

Several studies have demonstrated the functional significance of specific vein arrangements in insect wings. For example, the pleated, grid-like arrangement of leading edge veins in dragonfly wings helps strengthen the wing to spanwise bending (Newman and Wootton, 1986; Wootton, 1991), posteriorly curved veins in flies generate chordwise camber when a force is applied to the wing (Ennos, 1988), and the fan-like distribution of veins in the locust hindwing causes the wing margin to bend downward when the wing is extended (Herbert et al., 2000; Wootton, 1995; Wootton et al., 2000). Beyond these specialized mechanisms, however, the functional significance of the enormous differences in overall venation pattern in insect wings remains unclear.

Given the large phylogenetic changes in cross-venation, vein

diameter and spatial distribution of veins (Fig. 1), one might expect insect wings to display large mechanical differences that would affect their deformability during flight. On the other hand, differences in venation pattern may reflect alternative designs that provide insect wings with similar overall mechanical and bending properties while allowing veins to be rearranged for other reasons.

Quantitative measurements of wing stiffness that would allow one to distinguish between these hypotheses remain limited to a small number of studies. Wing stiffness has been assessed by applying point forces to isolated wing sections, in dragonflies (Newman and Wootton, 1986) and locusts (Wootton et al., 2000), or at the center of pressure to produce torsion, in flies (Ennos, 1988) and butterflies (Wootton, 1993). Steppan (2000) measured bending stiffness in dried butterfly wings, and Smith et al. (2000) measured material stiffness (Young's modulus, *E*) of insect wing membrane from locust hindwings. Although each of these studies provides insight into the functional wing morphology of the species examined, the measurements are difficult to compare in a broader phylogenetic context because of variations in technique.

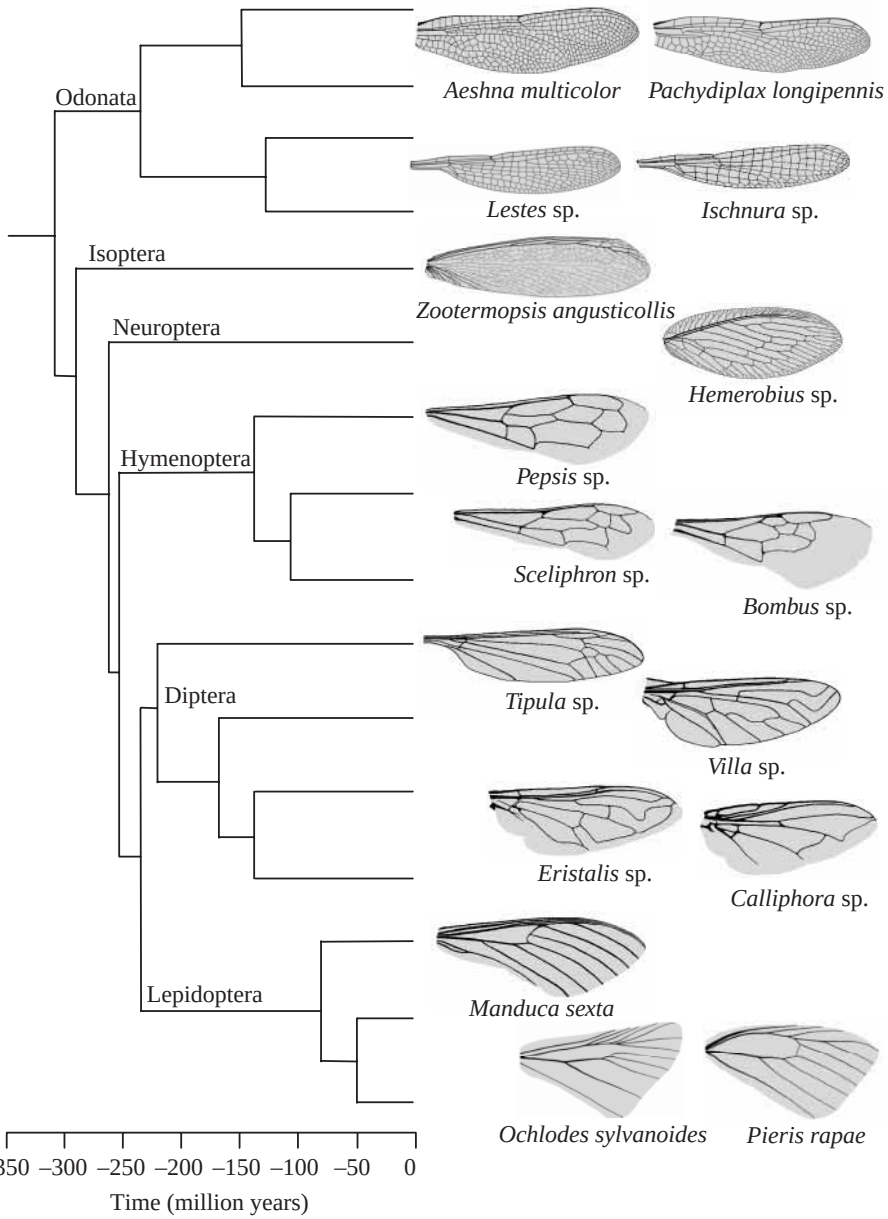

Fig. 1. Drawings of forewings from insects used in this study, arranged on the phylogenetic tree used to calculate independent contrasts. Veins are drawn at actual thickness; wings are not shown to scale. Genus and species names (when known) are shown under each wing, and orders are listed at their branching points. Branching and divergence dates of orders were derived from Kristensen (1991), Kukalova-Peck (1991), Whiting et al. (1997) and Wootton (1990b). Branching patterns and divergence dates within orders were derived from Benton (1993), Maddison (1995a,b), Trueman and Rowe (2001) and Wiegmann and Yeates (1996).

In this study, we examined the relationship between insect wing flexibility and venation by measuring flexural stiffness (*EI*) and quantifying venation pattern in 16 insect species from six orders. Flexural stiffness is a composite measure of the overall bending stiffness of a wing; it is the product of the material stiffness (*E*, which describes the stiffness of the wing material itself) and the second moment of area (*I*, which describes the stiffness generated by the cross-sectional geometry of the wing). Because insect wings bend spanwise (from wing base to wing tip) and chordwise (from leading to trailing edge) during flight, we measured flexural stiffness in both of these directions.

Correlations between venation pattern and wing flexural stiffness may arise either from a functional relationship between these traits or simply as a result of the shared phylogenetic history of the species examined. To remove the effects of phylogeny from this study, we calculated standardized independent contrasts (Felsenstein, 1985; Garland et al., 1999) of venation and stiffness measurements, and examined the correlations between these contrasts to assess the relationship between wing venation pattern and flexural stiffness.

Finally, we created a simplified finite element model of an insect wing, in which we can alter the stiffness of specific wing veins (or remove veins entirely) and perform numerical experiments to assess the resulting flexural stiffness of the whole wing. This

modeling approach allows us to examine the functional significance of various wing veins in generating the overall patterns of flexural stiffness measured in real wings.

Materials and methods

Insect collection and handling

We measured flexural stiffness and wing venation pattern in the forewings of 16 insect species from six orders: Odonata (two dragonfly and two damselfly), Isoptera (termite), Neuroptera (lacewing), Hymenoptera (two wasp and one bee), Diptera (four flies from different families) and Lepidoptera (two butterfly and one hawkmoth); see Fig. 1 for species names. We measured spanwise and chordwise flexural stiffness in 2–10 individuals of each species, depending on availability.

Insects were collected locally or obtained from laboratory colonies and placed in a humidified container at 4°C until experiments were performed. Within 1 week of capture, we cold-anaesthetized an insect, recorded its mass, removed one forewing, and placed the insect back in the humidified container. We photographed the wing and measured its flexural stiffness in the spanwise direction within 1 h of removing the wing from the insect (during which time the stiffness of the wing does not change appreciably, according to trials). We then repeated this process for the other forewing, measuring flexural stiffness in the chordwise direction.

Flexural stiffness measurements

We measured flexural stiffness of wings by applying a point force to bend the wing in either the spanwise or chordwise direction, and using the measured force and wing displacement to calculate overall flexural stiffness *EI* with a beam equation (see below). We glued wings to glass slides using cyanoacrylate glue cured with baking soda, at either the wing base (for spanwise measurements) or the leading edge (for chordwise measurements; Fig. 2A). We then fixed the slide to the left side of the apparatus shown in Fig. 2B and adjusted the right arm so that the pin contacted the wing on its dorsal surface. We applied the point force at 70% of wing span or chord length because the pin slipped from the wing if it was placed too close to the edge. We performed four measurements with point loads of varying magnitude, lowering the right side of the apparatus with a micrometer, measuring force and displacement and returning to the zero (unloaded) position between each measurement. We then flipped the slide over and repeated the measurements, loading the wing from the ventral side.

We removed the slide and measured the distance from the point of wing attachment to the point of force application to determine the effective beam length (*L*). We calculated *EI* over this distance as in Gordon (1978):

$$EI = FL^3 / 3\delta , \quad (1)$$

where *F* is applied force and δ is wing displacement at the point of force application (70% span or chord). This equation provides a measure of the flexural stiffness over the entire beam length, and assumes that the beam is homogeneous (see Discussion for an analysis of the beam equation assumptions). Because the equation applies only to small displacements, we removed any measurements where wing displacement was more than 5% of the effective beam length (where $\delta > 0.05L$). We averaged the repeated measurements on each side into a single dorsal and a single ventral value and tested for a significant difference ($P<0.05$) between dorsal and ventral values with a Wilcoxon signed rank test.

We plotted spanwise and chordwise flexural stiffness against several measures of wing and body size: wing span and maximum chord length (measured in NIH Image), wing area (measured in Matlab; see below) and body mass. We also combined these size measurements using principal components analysis into a measure of overall size (including all four variables) and a measure of wing size (including wing span, chord and area).

To verify our technique for measuring *EI*, we measured

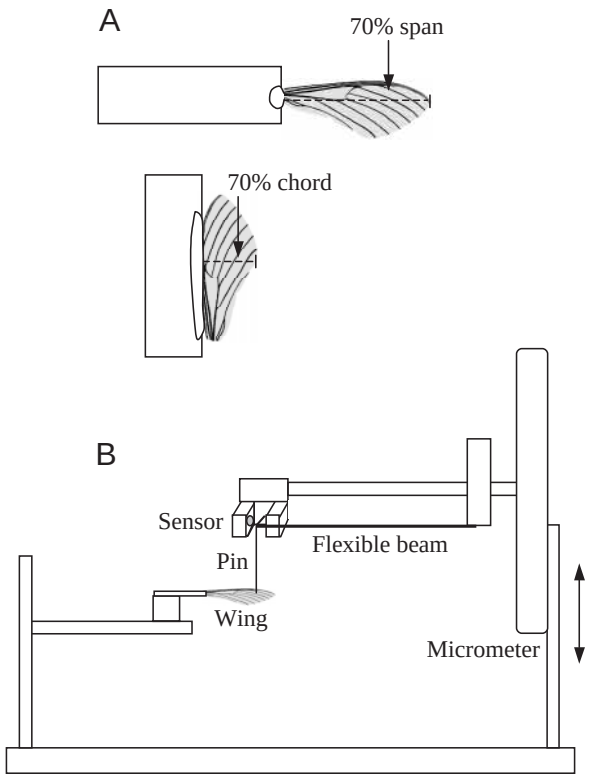

Fig. 2. Method used to measure insect wing displacement in response to an applied force. (A) For spanwise measurements, point forces were applied at approximately 70% of wing span, near the leading edge (top). For chordwise measurements, point forces were applied at 70% of chord length, midway between the wing base and tip (bottom). (B) Wings were fixed to the left side of the apparatus, and the right side was lowered until a pin attached to a flexible beam contacted the wing. A micrometer was then used to lower the right arm by a known distance, applying a point force that moved the wing down and the flexible beam up. The motion of the beam was recorded *via* an optical sensor, and used to calculate the applied force and displacement of the wing.

force and displacement of a thin, rectangular glass coverslip (a homogeneous beam of linearly elastic material) at three different lengths (with 3, 4 and 4.85 cm of the coverslip extending past the point of attachment). We then calculated *EI* for each beam length, measured the thickness and width of the coverslip, and calculated *I*, the second moment of area as in Gordon (1978):

$$I = wt^3 / 12 , \quad (2)$$

where *w* is width and *t* is thickness. Finally, we compared the resulting value of *E*, Young's modulus, with a known value for glass (E=7×10^{10} N m^{-2}; Gordon, 1978).

Wing shape and venation measurements

From photographs of each wing, we created a black silhouette in Photoshop and used NIH Image to measure wing span and chord. For one wing of each species, we hand-digitized the wing veins in Photoshop so that both the position and precise diameter of the veins were represented (Fig. 1).

From the digitized vein images, we counted the number of vein intersections in each wing as a measure of the complexity of vein branching. We imported images of the wing silhouette and veins into Matlab and measured the planform area of the whole wing and of the wing veins. From these measurements, we calculated the vein density (proportion of planform wing area occupied by veins) as the planform vein area divided by total wing area. We also determined average vein thickness by finding the total length of veins in the wing (see Combes, 2002) and dividing planform vein area by total vein length. We divided this value by wing span to scale for overall wing size.

Finally, we measured two venation characteristics related to the leading edge of the wing: the proportion of veins in the leading edge and the density of veins in the leading edge. We defined the leading edge visually as a cohesive unit of veins running spanwise along the anterior edge of each wing (Combes, 2002). We imported digitized images of these leading edge veins and a silhouette of the leading edge area (leading edge veins plus the area they surround) into Matlab. We then calculated the proportion of veins in the leading edge as the leading edge vein area divided by total planform vein area, and calculated leading edge vein density as the leading edge vein area divided by the area of the leading edge silhouette.

Phylogenetic analysis of correlated characters

Because the species tested share a phylogenetic history, some characters (e.g. wing venation and flexural stiffness) may be correlated in closely related groups simply because these species share a common ancestor that possessed these characters, and not because the characters are related in any functional way. As a result, the species used in this study cannot be treated as independent data points for statistical analysis. However, any differences in traits between two adjacent (closely related) groups can be assumed to have occurred independently, after the two groups diverged. Therefore, we can calculate the independent contrasts (or differences) between values of a trait in adjacent groups, and plot the standardized contrasts of one trait against those of another to see if a relationship exists between the traits when the effect of phylogeny has been removed (Felsenstein, 1985; Garland et al., 1999).

We calculated independent contrasts of flexural stiffness and wing venation data using the Phenotypic Diversity Analysis Programs (PDAP), version 6.0, developed by Garland, Midford, Jones, Dickerman and Diaz-Uriarte [originally from Garland et al. (1993), with modifications in Garland et al. (1999) and Garland and Ives (2000)]. This program allows one to construct a phylogenetic tree and enter tip values for traits; it then calculates independent contrasts and performs various diagnostics on the output.

Some aspects of the phylogenetic relationships of the pterygotes (winged insects) are under debate, and the divergence times of groups and families are far from certain. However, we constructed a phylogeny of the species used in this study by combining the available information, and in some cases averaging or choosing midpoints between estimates of branching times in the phylogeny (Fig. 1). To determine how sensitive the analysis is to phylogenetic branch length, we also calculated independent contrasts using arbitrary branch lengths (Pagel, 1992), in which all internode branches are equal to one, but the tips of the tree are contemporaneous. We tested for correlations between standardized contrasts in JMP 4 on a Macintosh computer.

Finite element modeling

To explore how wing veins contribute to the flexural stiffness of a wing, we used MSC Marc/Mentat to create a simplified finite element model of an insect wing based on the *Manduca* wing shown in Fig. 1. Our goal was not to reproduce the behavior of a real *Manduca* wing, but rather to create a general model of a wing to explore how simply adding or strengthening veins in certain regions of the wing affects the overall flexural stiffness of the structure. Therefore, we did not attempt to recreate the precise three-dimensional shape of a *Manduca* wing (including changes in membrane thickness, vein cross-sectional shape and vein/membrane attachments), but instead modeled the wing as a flat plate of uniform thickness, composed of thin shell elements arranged to mimic the planform shape and vein configuration of a *Manduca* wing (Fig. 3A).

This generalized model allowed us to increase the stiffness of various groups of veins beyond that of the surrounding membrane to determine how these veins contribute to overall wing flexural stiffness. The flexural stiffness of individual veins in real insect wings is determined by both their geometric properties (generally those of hollow tubes) and the material properties of their walls. A hollow tube has a second moment of area *I* that can be several orders of magnitude higher than that of a flat plate of the same width (and equivalent wall thickness). Because our model is composed solely of flat elements (with a lower second moment of area), we adjusted

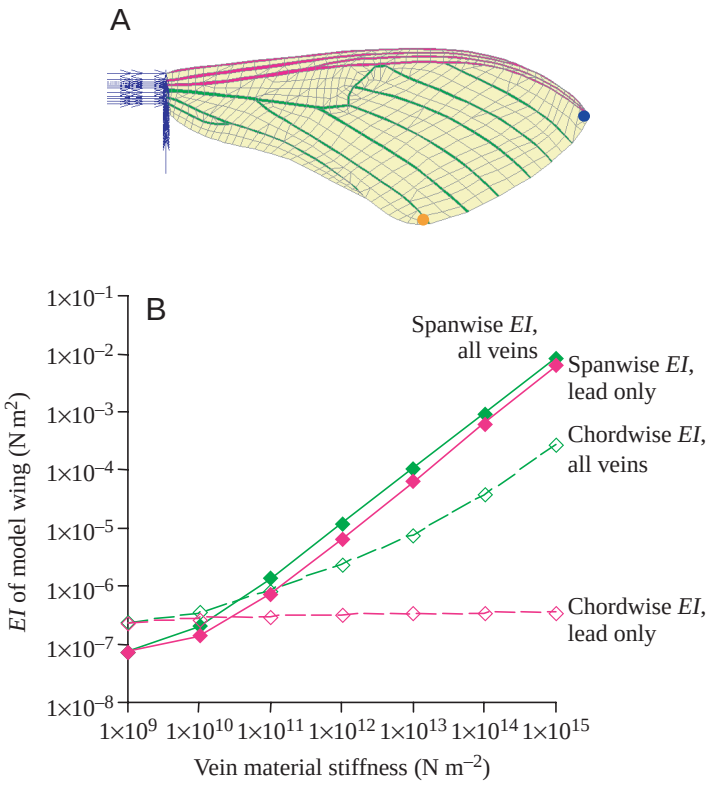

Fig. 3. Finite element model of an insect wing and results of virtual bending experiments. (A) Finite element model (FEM) based on the forewing of *Manduca sexta*, with leading edge vein elements in pink, other vein elements in green and membrane elements in yellow. (B) FEM wing flexural stiffness *EI* (calculated from applied force and wing displacement) *versus* material stiffness *E* of vein elements. In all simulations, the material stiffness of the membrane elements was 1×10^9 N m^{-2}. For results shown in green, the material stiffness of all vein elements was increased; for results shown in pink, the material stiffness of only leading edge vein elements was increased (while other vein elements remained at 1×10^9 N m^{-2}). Filled symbols, spanwise *EI*; open symbols, chordwise *EI*.

the flexural stiffness of the veins by increasing the material stiffness (*E*, Young's modulus) of these elements beyond that of the surrounding membrane elements.

We chose an element density of 1200 kg m^{-3} (as measured in insect wings; Wainwright et al., 1982) and an element thickness of 45 μm. We used a Poisson's ratio of 0.49, as measured in some biological materials (Wainwright et al., 1982); because the Poisson's ratio of insect wings is unknown, we tested the effects of using a Poisson's ratio of 0.3 and found that the difference in model behavior was negligible. To determine the minimum number of elements needed, we performed a sensitivity analysis with models composed of 200, 350, 865 and 2300 total elements, and found that 865 elements are sufficient to ensure asymptotic performance of the model.

We subjected the model wing to virtual static bending tests that mimic the tests performed on actual wings, fixing the base with zero displacement or rotation and applying a point force to the wing tip (Fig. 3A, blue dot). The model calculates the tip displacement due to this point force (and given the material properties of the membrane and veins). We then used the applied force, displacement, and wing span to calculate overall spanwise *EI* for the model wing as above (Equation 1). Similarly, we fixed the model wing at the leading edge and applied a point force at the trailing edge (Fig. 3A, orange dot) to calculate chordwise flexural stiffness.

In all simulations, we used a material stiffness of 1×10^9 N m^{-2} for the membrane elements (as measured in locust wings; Smith et al., 2000). In the first set of simulations, we used a material stiffness of 1×10^9 N m^{-2} for the vein elements as well (thus the wing was essentially veinless in these simulations). We then increased the material stiffness of the vein elements by orders of magnitude up to 1×10^{15} N m^{-2}, while membrane stiffness remained at 1×10^9 N m^{-2}. This increased vein material stiffness represents not only potential differences in the material properties of wing veins and membrane, but also differences in the second moment of area caused by the three-dimensional shape of veins. To test the effect of leading edge veins alone, we increased the material stiffness of the leading edge veins (in pink, Fig. 3A) by orders of magnitude to 1×10^{15} N m^{-2}, while fixing the material stiffness of the remaining vein and membrane elements at 1×10^9 N m^{-2}.

To validate our finite element modeling approach, we created a model of the glass coverslip used as an experimental control. We attached the coverslip at its base, with 4.85 cm of the coverslip extending past the point of attachment, and used a Young's modulus for glass of 7×10^{10} N m^{-2} (Gordon, 1978). We applied a series of point forces to the tip of the coverslip (equivalent to those applied in the experiment) and compared the tip displacements predicted by the model to those measured in the experiment.

Results

Flexural stiffness measurements

The glass coverslip used as a control had a second moment of area (*I*) of 6.75×10^{-15} m^4. Dividing the measured values of *EI* by *I* provided estimates of 7.3×10^{10}, 6.9×10^{10}, and 7.5×10^{10} N m^{-2} for the material stiffness (*E*) of the slide at beam lengths of 3, 4 and 4.85 cm, respectively. These values are close to the reported material stiffness of ordinary glass, 7×10^{10} N m^{-2} (Gordon, 1978).

The measurements of overall wing flexural stiffness in this study did not reveal a significant dorsal–ventral difference in the spanwise or chordwise direction in any species tested; we therefore averaged dorsal and ventral meaurements of *EI* in each direction. These flexural stiffness measurements were significantly correlated with all size variables tested (see Combes, 2002). However, spanwise stiffness was more strongly correlated with wing span (r^2=0.95; Fig. 4A) than

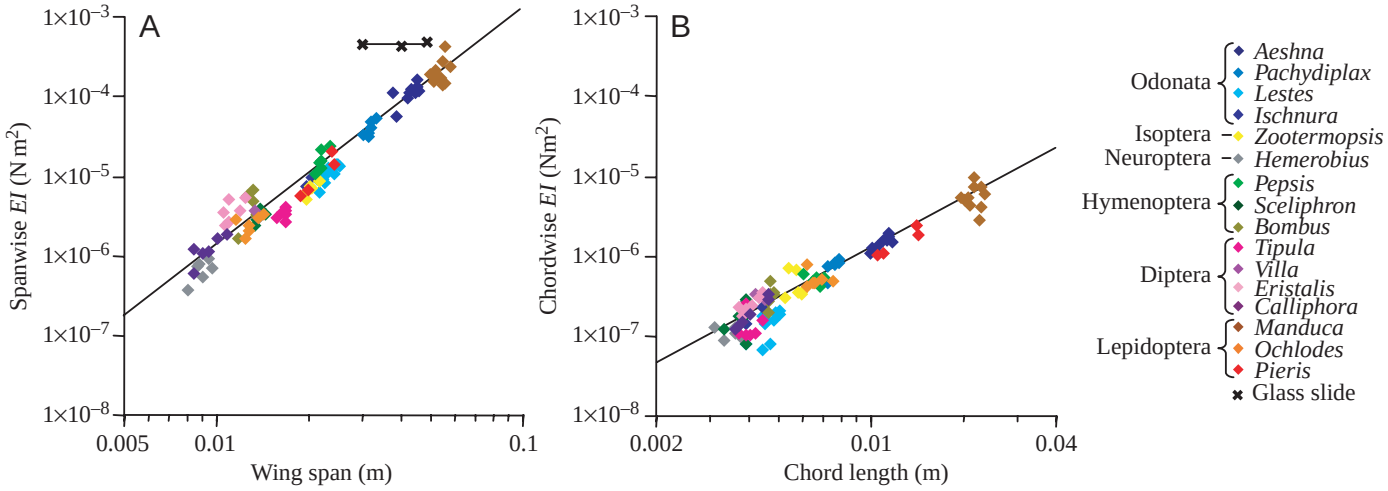

Fig. 4. Flexural stiffness *versus* span/chord length in 16 insect species. Individuals of each species are plotted in the same color. Axes are on a logarithmic scale. (A) Spanwise flexural stiffness *EI versus* wing span; for log–log transformed data, $y=2.97x+0.08$, $r^2=0.95$ (using species averages, $y=2.93x+0.03$, $r^2=0.96$). Measured flexural stiffness of a glass coverslip (at varying lengths) is shown in black. (B) Chordwise flexural stiffness *EI versus* chord length; for log–log transformed data $y=2.08x–1.73$, $r^2=0.91$ (using species averages, $y=2.01x–1.8$, $r^2=0.96$).

with any other size variable, or with the principal components of wing or body size. Similarly, chordwise stiffness was most strongly correlated with chord length ($r^2=0.91$; Fig. 4B). The measurements of flexural stiffness also revealed a large anisotropy in all species tested, with spanwise flexural stiffness approximately 1–2 orders of magnitude larger than chordwise flexural stiffness (Fig. 4).

Phylogenetic analysis of correlated characters

To verify that the correlations between flexural stiffness and size remain significant when the effect of phylogeny is removed, we calculated standardized independent contrasts of log-transformed spanwise *EI*, wing span, chordwise *EI* and chord length. The relationships between standardized independent contrasts of these wing size and flexural stiffness traits were significant, and the slopes were nearly the same as in the original data (span: $y=3.04x$, $r^2=0.96$; chord: $y=2.02x$, $r^2=0.96$). The residuals from these relationships can be used as an estimate of flexural stiffness with the effect of size (and phylogeny) removed (for examples of similar uses in correcting for body size, see Garland and Janis, 1993; Rezende et al., 2002).

These size-corrected estimates of flexural stiffness were not significantly correlated with standardized independent contrasts of any of the five wing venation characters measured. However, the residual of spanwise flexural stiffness was positively correlated with the residual of chordwise flexural stiffness ($r^2=0.37$, $P=0.012$), and several contrasts of vein characters were correlated with each other (Combes, 2002). When Pagel's arbitrary phylogenetic branch lengths (Pagel, 1992) were used, the residuals of flexural stiffness remained uncorrelated with wing venation characters, and the residuals of spanwise and chordwise flexural stiffness remained positively correlated (Combes, 2002).

Finite element modeling

The model of the glass coverslip provided estimates of tip displacement that were within 5% of those measured in the experiments, validating the finite element method. Virtual static bending tests of the model wing showed that chordwise flexural stiffness was higher than spanwise flexural stiffness when no veins were present (when membrane and vein material stiffness were the same; Fig. 3B). However, when veins were added and their material stiffness was increased, spanwise flexural stiffness increased beyond chordwise flexural stiffness. When only leading edge veins were added, spanwise flexural stiffness increased as above, while chordwise flexural stiffness did not change significantly from the veinless model (Fig. 3B).

Discussion

Our measurements of overall flexural stiffness in insect wings demonstrate that flexural stiffness varies widely in the species tested, but is strongly correlated with wing size. In fact, the span or chord length of a wing accounts for over 95% of the variability in spanwise and chordwise flexural stiffness, when the effects of phylogeny have been removed. Because flexural stiffness is a length-independent measure (for example, *EI* does not change significantly in glass coverslips over a range of lengths; Fig. 4A), these results suggest that there is a strong scaling relationship between wing size and flexural stiffness.

This strong relationship is apparent despite several assumptions inherent in the use of a homogeneous beam equation (Equation 1). Because wings resemble plates more closely than beams, we used simple finite element models to assess how robust the beam equation is to variations in the shape of the beam. We created models of rectangular plates

spanning the size and flexural stiffness range measured in real wings, applied point forces at the free end, and recorded the displacement of the model plate. We then calculated *EI* using Equation 1 and compared this to the known *EI* of the plate (based on its cross-sectional dimensions and material stiffness). We found that Equation 1 slightly overestimates flexural stiffness (by up to 12%) when the plate is longer than it is wide (i.e. for wings measured in the spanwise direction), and underestimates flexural stiffness (by up to 80%) when plates are wider than they are long. However, there is no overall trend in wing shape with increasing span or chord length, and these changes in *EI* are relatively small compared to the large range of flexural stiffness measured both within and between species (Fig. 4).

We also used the finite element model of an insect wing to explore the effects of inherent wing camber on flexural stiffness estimates. The maximum camber measured in *Manduca* wings with a laser ranging technique (see Combes and Daniel, 2003a) was 5% in the chordwise direction and 4% in the spanwise direction. Applying these levels of camber to the model wing had almost no effect on displacement when the wing was cambered parallel to the wing attachment (i.e. when the model wing was cambered in the chordwise direction and chordwise flexural stiffness was measured). When the wing was cambered in the direction perpendicular to the attachment (i.e. when the wing was cambered in the spanwise direction and chordwise flexural stiffness was measured), displacement varied up to a maximum of 40% from the value measured in a flat plate, indicating a relatively minor effect on flexural stiffness.

Finally, the assumption in Equation 1 that flexural stiffness is homogeneous across a wing may lead to a systematic error in the reported values, which could potentially underlie the observed scaling relationships. If flexural stiffness varies along the wing span or chord, the reported values of overall flexural stiffness represent some weighted integration of *EI* along the length measured. If this integral varies systematically as beam length increases, it could account for part of the size scaling in the data. We explored this hypothesis numerically by integrating various simple functions (that represent how stiffness might vary in the wing) over increasing beam length. We found that the integral of *EI* over the wing may vary slightly with length depending on the function used, but this variation is far smaller than the range of values measured in real wings, and is therefore unlikely to cause the observed scaling relationships (Combes, 2002).

Scaling of flexural stiffness

The strong correlations between wing size and flexural stiffness suggest that size scaling is the dominant factor determining overall flexural stiffness in insect wings. Because *EI* is a composite measure that incorporates the second moment of area as well as the material stiffness of a wing, it is not surprising that spanwise and chordwise flexural stiffness increase with wing size; wings with larger spans generally also have larger average chord lengths (and thus *I*, the second moment of area, is higher). *I* is proportional to a beam's width times its thickness cubed (Equation 2). For measurements of spanwise flexural stiffness, the width of the beam is the average chord length, and in the species tested average chord length is directly proportional to wing span (y=0.2546x–0.0004, r^2=0.8574). The average thickness of the wings tested, however, is unknown. Average thickness may be proportional to span (if wings grow isometrically), or could be independent of span (since all cuticle consists of a single cell layer with extracellular deposits). If we assume that *E*, the material stiffness of wing cuticle, does not vary with wing size, we would predict that flexural stiffness should scale with length (if thickness is independent of span) or with length to the fourth power (if thickness is directly proportional to span). The results of this study do not agree with either of these predictions; spanwise *EI* scales with the cube of chord length, whereas chordwise *EI* scales with the square of span. Thus, increased second moment of area alone cannot account for the observed scaling of spanwise and chordwise flexural stiffness.

Scaling of flexural stiffness has been examined previously in dried butterfly wings (Steppan, 2000) and in the primary flight feathers of birds (Worcester, 1996), both of which show a positive correlation between flexural stiffness and size. The authors compared the observed scaling relationships with the theory of geometric similarity (see Alexander et al., 1979), where structures maintain a similar shape regardless of size, as well as with the theory of elastic similarity (see McMahon, 1973), in which loaded structures maintain a similar angular deflection regardless of size. Neither study (Steppan, 2000; Worcester, 1996) found scaling patterns that could be explained by geometric similarity, and the results of our work appear to agree with these conclusions. The exponents of the relationship between insect wing flexural stiffness and body mass (0.91 spanwise and 0.61 chordwise; Combes, 2002) are far from the expected value of 1.67 proposed by Worcester (1996) for geometric similarity, and the exponents of the relationship between flexural stiffness and wing area (1.50 spanwise and 0.99 chordwise; Combes, 2002) are also far from the expected value of 2.0 proposed by Steppan (2000).

If the scaling of wing flexural stiffness provides functional, rather than geometric similarity across a range of body sizes, wing angular deflection should remain constant, as in elastic similarity (McMahon, 1973). If we take tip displacement divided by wing span (or trailing edge displacement divided by chord length) as a rough measure of strain or curvature in the wing, we can rearrange Equation 1 as:

$$\delta / L = FL^2 / EI \,. \quad (3)$$

Spanwise flexural stiffness scales with L^3 and chordwise flexural stiffness with L^2. This suggests that in the chordwise direction, δ/L is directly proportional to force, regardless of the chord length of the wing. In the spanwise direction, δ/L is proportional to F/L, so spanwise curvature would be smaller in large wings for a given force.

To assess whether δ/L remains constant in flying insects over a range of sizes, we need to know how the forces on flapping

insect wings scale with size. If we assume that the primary forces on an insect's wings are aerodynamic, then force is proportional to body mass. However, several studies have suggested that the inertial forces generated by flapping wings may be considerably larger than the aerodynamic forces (Combes and Daniel, 2003b; Daniel and Combes, 2002; Ellington, 1984; Ennos, 1989; Lehmann and Dickinson, 1997; Zanker and Gotz, 1990), and therefore inertial forces may be more important in determining wing deformations. A generalized scaling argument for inertial force in insect wings is difficult to derive because wingbeat frequency does not scale strongly with size in the insects studied here. However, small insects often have significantly higher wingbeat frequencies, so the ratio of inertial to aerodynamic forces acting on their wings may be as high or higher than in large insects with heavier (but slower) wings (Combes and Daniel, 2003b; Daniel and Combes, 2002).

Effects of wing venation on flexural stiffness

Although both spanwise and chordwise flexural stiffness scale with wing length, the magnitude of flexural stiffness in these directions differs greatly; spanwise *EI* is approximately 1–2 orders of magnitude higher than chordwise *EI* in all species tested (Fig. 4). Because spanwise flexural stiffness increases as L^3 and chordwise flexural stiffness only as L^2, this anisotropy is generally bigger in larger-winged insects.

The finite element analysis of an insect wing shows that this structural anisotropy is due to a common venation feature of insect wings: leading edge veins. The model without any strengthening veins demonstrates that the basic planform shape of the wing would lead to similar spanwise and chordwise flexural stiffness if no veins were present (Fig. 3B). Adding leading edge veins to the model increases spanwise flexural stiffness dramatically, generating spanwise–chordwise anisotropy (Fig. 3B).

Clustered or thickened veins in the leading edge of the wing are found in nearly all insects, even insects that have lost all other wing veins (such as some hymenopterans and small dipterans). Thus, spanwise–chordwise anisotropy may be a universal trait among insects. This anisotropy would serve to strengthen the wing from bending in the spanwise direction while allowing chordwise bending to generate camber. It could also facilitate spanwise torsion, which is seen in many species during supination (Ennos, 1988; Wootton, 1981).

Although leading edge veins appear to play a crucial role in determining the relative magnitudes of spanwise and chordwise flexural stiffness, the details of venation pattern measured in this study do not appear to affect the overall flexural stiffness of the wing. We did find, however, that the residuals of spanwise flexural stiffness are correlated with the residuals of chordwise flexural stiffness. This indicates that some insects have wings that are generally stiffer (in both directions) than expected for their size, while others have wings that are more flexible than expected. The residuals from the original data show that dragonflies, hawkmoths, flies (except for craneflies) and bumblebees all have wings that are stiffer than expected for their size. Damselflies, craneflies and lacewings have more flexible wings than expected, while butterflies and wasps are intermediate.

The functional significance of phylogenetic changes in wing venation (such as loss of cross veins and increased vein thickness) remains unclear. Perhaps more derived groups of insects have simply evolved a venation pattern that allows them to maintain the essential scaling of wing stiffness in a more economical way (e.g. using less vein material), or perhaps the venation patterns are related to something entirely different, such as the distribution of sensory receptors on the wing (Kammer, 1985).

Alternatively, venation pattern may in fact affect wing stiffness, but in ways that could not be detected in this study. For example, venation pattern may not affect overall stiffness, but could influence how stiffness varies throughout the wing (see Combes and Daniel, 2003a). In addition, the stiffness measurements in this study exclude the outer 30% of the wing, which is likely to be the most flexible region. Differences in wing stiffness between insects with veins that extend to and delineate the trailing edge (such as odonates; see Fig. 1) and insects with primarily unsupported membrane in the trailing edge (such as hymenopterans) would most likely be found in this region. How the spatial distribution of stiffness contributes to the instantaneous shape of a dynamically moving wing is a subject of further study, and will be crucial to understanding the implications of mechanical design of wings to insect flight performance.

List of symbols

EI	flexural stiffness
E	material stiffness (Young's modulus)
I	second moment of area
L	effective beam length
F	applied force
δ	wing displacement at the point of force application
w	width
t	thickness

R. Sugg and J. Edwards graciously assisted in identifying the insects used in this study. D. O'Carroll, T. Morse and J. Kingsolver provided specimens, and D. Combes assisted in collecting and transporting the spiderwasps. T. Garland provided the program for calculating independent contrasts, as well as helpful advice on its use. D. Grunbaum and R. Huey contributed useful comments on both the project and drafts of the paper. This work was supported by NSF grant F094801 to T.D., the John D. and Catherine T. MacArthur Foundation, an NSF graduate fellowship to S.C. and an ARCS fellowship to S.C.

References

Alexander, R. McN., Jayes, A. S., Maloiy, G. M. O. and Wathuta, E. M. (1979). Allometry of the limb bones of mammals from shrews (*Sorex*) to elephant (*Loxodonta*). *J. Zool., Lond.* **189**, 305-314.

Benton, M. J. (ed.) (1993). *The Fossil Record 2*, 845pp. London: Chapman & Hall. *http://palaeo.gly.bris.ac.uk/frwhole/FR2.html*

Borror, D. J., Triplehorn, C. A. and Johnson, N. F. (1989). *An Introduction to the Study of Insects*, 6th edition. Fort Worth, TX: Harcourt Brace College Publishers.

Combes, S. A. (2002). Wing flexibility and design for animal flight. PhD thesis, University of Washington, USA.

Combes, S. A. and Daniel, T. L. (2003a). Flexural stiffness in insect wings. II. Spatial distribution and dynamic wing bending. *J. Exp. Biol.* **206**, 2989-2997.

Combes, S. A. and Daniel, T. L. (2003b). Into thin air: Contributions of aerodynamic and inertial-elastic forces to wing bending in the hawkmoth *Manduca sexta*. *J. Exp. Biol.* **206**, 2999-3006.

Dalton, S. (1975). *Borne On The Wind: The Extraordinary World of Insects in Flight*. New York: Reader's Digest Press.

Daniel, T. L. and Combes, S. A. (2002). Flexing wings and fins: bending by inertial or fluid-dynamic forces? *Int. Comp. Biol.* **42**, 1044-1049.

Ellington, C. P. (1984). The aerodynamics of hovering insect flight. Part VI: Lift and power requirements. *Phil. Trans. R. Soc. Lond. B* **305**, 145-181.

Ennos, A. R. (1988). The importance of torsion in the design of insect wings. *J. Exp. Biol.* **140**, 137-160.

Ennos, A. R. (1989). Inertial and aerodynamic torques on the wings of Diptera in flight. *J. Exp. Biol.* **142**, 87-95.

Felsenstein, J. (1985). Phylogenies and the comparative method. *Am. Nat.* **125**, 1-15.

Garland, T., Jr, Dickerman, A. W., Janis, C. M. and Jones, J. A. (1993). Phylogenetic analysis of covariance by computer simulation. *Syst. Biol.* **42**, 265-292.

Garland, T., Jr, Midford, P. E. and Ives, A. R. (1999). An introduction to phylogenetically based statistical methods, with a new method for confidence intervals on ancestral states. *Am. Zool.* **39**, 374-388.

Garland, T., Jr and Ives, A. R. (2000). Using the past to predict the present: Confidence intervals for regression equations in phylogenetic comparative methods. *Am. Nat.* **155**, 346-364.

Garland, T., Jr and Janis, C. M. (1993). Does metatarsal/femur ratio predict maximal running speed in cursorial mammals? *J. Zool., Lond.* **229**, 133-151.

Gordon, J. E. (1978). *Structures: or Why Things Don't Fall Down*. New York: Penguin Books.

Herbert, R. C., Young, P. G., Smith, C. W., Wootton, R. J. and Evans, K. E. (2000). The hind wing of the desert locust (*Schistocerca gregaria* Forskål). III. A finite element analysis of a deployable structure. *J. Exp. Biol.* **203**, 2945-2955.

Kammer, A. E. (1985). Flying. In *Comprehensive Insect Physiology, Biochemistry and Pharmacology*. Vol. 5, *Nervous system: structure and motor function* (ed. G. A. Kerkut and L. I. Gilbert), pp. 491-552. Oxford: Pergamon Press.

Kent, G. C. (1992). *Comparative Anatomy of the Vertebrates*. St Louis, Missouri: Mosby-Year Book, Inc.

Kristensen, N. P. (1991). Phylogeny of extant hexapods. In *The Insects of Australia: A textbook for students and research workers*, 2nd edition, Vol. 1, pp. 125-140. Ithaca, NY: Cornell University Press.

Kukalova-Peck, J. (1991). Fossil history and the evolution of hexapod structures. In *The Insects of Australia: A textbook for students and research workers*, 2nd edition, vol. 1, pp. 141-179. Ithaca, NY: Cornell University Press.

Lehmann, F.-O. and Dickinson, M. H. (1997). The changes in power requirements and muscle efficiency during elevated force production in the fruit fly *Drosophila melanogaster*. *J. Exp. Biol.* **200**, 1133-1143.

Maddison, D. R. (1995a). Hymenoptera. In *The Tree of Life Web Project*, (ed. D. R. Maddison and K.-S. Schultz). *http://tolweb.org/tree/phylogeny.html*

Maddison, D. R. (1995b). Lepidoptera. In *The Tree of Life Web Project*, (ed. D. R. Maddison and K.-S. Schultz). *http://tolweb.org/tree/phylogeny.html*

McMahon, T. A. (1973). Size and shape in biology. *Science* **179**, 1201-1204.

Newman, D. J. S. and Wootton, R. J. (1986). An approach to the mechanics of pleating in dragonfly wings. *J. Exp. Biol.* **125**, 361-372.

Pagel, M. D. (1992). A method for the analysis of comparative data. *J. Theor. Biol.* **164**, 194-205.

Rezende, E. L., Swanson, D. L., Novoa, F. F. and Bozinovic, F. (2002). Passerines *versus* nonpasserines: so far, no statistical differences in the scaling of avian energetics. *J. Exp. Biol.* **205**, 101-107.

Smith, C. W., Herbert, R., Wootton, R. J. and Evans, K. E. (2000). The hind wing of the desert locust (*Schistocerca gregaria* Forskål). II. Mechanical properties and functioning of the membrane. *J. Exp. Biol.* **203**, 2933-2943.

Steppan, S. J. (2000). Flexural stiffness patterns of butterfly wings (Papilionoidea). *J. Res. Lepid.* **35**, 61-77.

Trueman, J. W. H. and Rowe, R. J. (2001). Odonata. In *The Tree of Life Web Project* (ed. D. R. Maddison and K.-S. Schultz). *http://tolweb.org/tree/phylogeny.html*

Wainwright, S. A., Biggs, W. D., Currey, J. D. and Gosline, J. M. (1982). *Mechanical Design in Organisms*. Princeton, New Jersey: Princeton University Press.

Whiting, M. F., Carpenter, J. C., Wheeler, Q. D. and Wheeler, W. C. (1997). The Strepsiptera problem: Phylogeny of the holometabolous insect orders inferred from 18s and 28s ribosomal DNA sequences and morphology. *Syst. Biol.* **46**, 1-68.

Wiegmann, B. M. and Yeates, D. K. (1996). Diptera. In *The Tree of Life Web Project* (ed. D. R. Maddison and K.-S. Schultz). *http://tolweb.org/tree/phylogeny.html*

Wootton, R. J. (1981). Support and deformability in insect wings. *J. Zool., Lond.* **193**, 447-468.

Wootton, R. J. (1990a). The mechanical design of insect wings. *Sci. Am.* **November**, 114-120.

Wootton, R. J. (1990b). Major insect radiations. In *Major Evolutionary Radiations*, Systematics Association Special Volume No. 42 (ed. P. D. Taylor and G. P. Larwood), pp. 187-208. Oxford: Clarendon Press.

Wootton, R. J. (1991). The functional morphology of the wings of Odonata. *Adv. Odonatol.* **5**, 153-169.

Wootton, R. J. (1992). Functional morphology of insect wings. *Annu. Rev. Entomol.* **37**, 113-140.

Wootton, R. J. (1993). Leading edge section and asymmetric twisting in the wings of flying butterflies (Insecta, Papilionoidea). *J. Exp. Biol.* **180**, 105-117.

Wootton, R. J. (1995). Geometry and mechanics of insect hindwing fans: a modelling approach. *Proc. R. Soc. Lond. B* **262**, 181-187.

Wootton, R. J., Evans, K. E., Herbert, R. and Smith, C. W. (2000). The hind wing of the desert locust (*Schistocerca gregaria* Forskål). I. Functional morphology and mode of operation. *J. Exp. Biol.* **203**, 2921-2931.

Worcester, S. E. (1996). The scaling of the size and stiffness of primary flight feathers. *J. Zool., Lond.* **239**, 609-624.

Zanker, J. M. and Gotz, K. G. (1990). The wing beat of *Drosophila melanogaster*. II. Dynamics. *Phil. Trans. R. Soc. Lond. B* **327**, 19-44.